

## **Chapter III**

# **Magnetic nanoparticles directed delivery of Berberine – A cytotoxic phytochemical, for tumor control**

**Chapter III: Magnetic nanoparticles directed delivery of Berberine -  
A cytotoxic phytochemical, for tumor control\***

**Table of Contents**

<b>3.1</b>	<b>Introduction</b>
<b>3.2</b>	<b>Materials and Methods</b>
3.2.1	<i>Animals</i>
3.2.2	<i>Chemicals</i>
3.2.3	<i>Preparation and characterization of NPs and NP-drug complexes</i>
3.2.4	<i>Experiment design</i>
3.2.5	<i>Tumor regression</i>
3.2.6	<i>Alkaline single cell gel electrophoresis</i>
3.2.7	<i>RNA isolation</i>
3.2.8	<i>Polymerase Chain Reaction</i>
3.2.9	<i>Morphology analysis</i>
3.2.10	<i>Hematology studies</i>
3.2.11	<i>Serum biochemical analysis</i>
3.2.12	<i>Statistical analysis</i>
<b>3.3</b>	<b>Results and Discussion</b>
3.3.1	<i>X-ray diffraction</i>
3.3.2	<i>Infra-Red Spectroscopy</i>
3.3.3	<i>Transmission Electron Microscopy</i>
3.3.4	<i>Analysis of tumor volume following the treatments to understand the anti-neoplastic activity of the treatments</i>
3.3.5	<i>Cellular DNA damage analysis on tumor, liver and blood</i>
3.3.6	<i>Analysis on the transcriptional level expression of genes related to apoptosis following the treatments</i>
3.3.7	<i>Analysis on histopathology of tumor and normal tissues following various treatments</i>
3.3.8	<i>Assessment on blood parameters of animals</i>
3.3.9	<i>Serum biomarkers of kidney and liver</i>
<b>3.4</b>	<b>Conclusion</b>

\*This chapter merited publication in the Journal of Advanced Science Engineering and Medicine as- Sreeja S, Nair CKK. Magnetic nanoparticles directed delivery of Berberine - a cytotoxic phytochemical, for tumor control. *Advanced Science Engineering and Medicine*, 2015; 7: 53-61.

In the present work iron oxide nanoparticles (NP(s)) were complexed with a cytotoxic isoquinoline alkaloid Berberine (BBN) and these complexes (NP-drug complexes) were targeted to the tumor site in mice-bearing solid tumor on hind limbs by the application of an external magnetic field. The NPs were characterized by FTIR, XRD and TEM. The tumor regression was studied and the mechanism of tumor regression was examined by comet assay, and both conventional and real time PCR. The morphological alterations of tissue ultra structure by histopathological examination, and blood and serum parameters of the treated animals were studied. The oral administration of NP-drug complexes along with external application of magnetic field resulted in significant reduction of tumor volume. The studies on both conventional and real time PCR revealed that the underlying molecular mechanism of the tumor regression was due to altered expression of the genes- *bax*, *bcl2*, *caspase 9*, *caspase 8* and *caspase 3*. The NP-drug complexes at the doses were found to be non-toxic as there was no change in the blood and serum biochemical parameters in the treated animals. Histopathological examinations indicated distinct alteration in the tumor tissues of treated animals while there was no change in normal tissues. The study suggests apoptosis through the intrinsic pathway could be the underlying mechanism of tumor regression by the magnetic NP directed delivery of BBN to the tumor cells.

### 3.1 INTRODUCTION

Particles in the nanoscale are revolutionizing various areas of science and technology including healthcare. Because of their unique properties such as small size (<100nm), large surface-to-volume ratio, longer circulation time, ability to reach target sites, they are effective in drug delivery. The phenomenon of Enhanced Permeability and Retention (EPR) Effect due to the leaky nature of blood vessels and lack of normal lymphatic drainage system in tumor, nanoparticles gets accumulated in tumor milieu and can reduce the exposure of drugs to normal healthy cells by limiting its distribution to the target [Khaled, 2007]. The surface modification of nanoparticles can inhibit the interaction of serum proteins and thereby prevent opsonisation and increase plasma half-life [Raju et al., 2011]. Thus, NPs of size less than 100nm is preferable for drug delivery in *in vivo* condition [Shundo et al., 2012; Cerdan et al., 1989].

NPs are of great importance in tumor therapy and diagnosis through imaging because of their biocompatibility and magnetic properties [Rivera et al., 2010]. The biocompatibility of NPs arises from the fact that ferric iron bind with transferrin and this complex can interact with cell surface transferrin receptor and transported to the cell cytoplasm. Within the cytoplasm, ferric irons are stored in proteins known as ferritin and hence considered to be less or non-toxic. NPs can be broken down to ferric iron and followed body's normal

iron metabolism [Nakamura et al., 2000]. The direction of movement of the NPs can be manipulated by the application of an external magnetic field [Neuberger et al., 2005; Mishima et al., 2007]. The applied magnetic field can navigate and accumulate nanoparticles to the tumor sites by controlling the strength of the magnetic field [Huang et al., 2012]. NPs are used as a potent platform for cancer therapy with the aid of both applied magnetic field and specific receptors [Mahmoudi et al., 2011].

Berberine chloride (2, 3-methylenedioxy-9, 10-dimethoxyprotoberberine Chloride; BBN) is an isoquinoline plant alkaloid found in *Berberis vulgaris* (barberry), *Berberis aquifolium* (Oregon grape), *Berberis aristata* (tree turmeric), *Phellodendron amurense* (Amur cork tree), *Hydrastis canadensis* (goldenseal) and *Xanthorrhiza simplicissima* (yellowroot). BBN has been used widely in Ayurvedic medicine as it possesses a large range of pharmacological and biochemical properties. It has revealed that BBN possesses anti-proliferative activity and is effective in cell cycle arrest and apoptosis induction in HeLa and L1210 cells [Jantova et al., 2003]. Iizuka et al., 2000 reported that treatment with BBN has an inhibitory effect on the proliferation of human esophageal cancer cell lines.

Though BBN exhibits higher anticancer properties, its insolubility in aqueous media is the hurdle in its application in anticancer treatments. The present work is an attempt to deliver cytotoxic drug BBN to tumor tissues in tumor-bearing animals with the help of magnetic nanoparticles and locally applied external magnetic field. Orally administered NP-BBN complexes enter into the cells of the tumors and are retained in these cells by the virtue of external magnetic field.

## **3.2 MATERIALS AND METHODS**

### **3.2.1 Animals**

Female *Swiss albino* mice weighing 22-25 g were obtained from the Small Animal Breeding Section (SABS), Mannuthy, Thrissur, Kerala. They were kept under standard conditions in the Centre's Animal House Facility. The animals were provided with standard mouse chow (Sai Durga Feeds and Foods, Bangalore, India) and water *ad-libitum*. All animal experiments in this study were carried out with the prior approval of the Institutional Animal Ethics Committee (IAEC) and were conducted strictly adhering to the guidelines of the Committee for the Purpose of Control and Supervision of

Experiments on Animals (CPCSEA) constituted by the Animal Welfare Division of Government of India.

### 3.2.2 *Chemicals*

Berberine chloride, Iron (III) chloride, Iron (II) chloride and Ammonium hydroxide solution were purchased from Sigma chemical company, USA. Other reagents were all of analytical grade and purchased from reputed Indian manufacturers.

### 3.2.3 *Preparation and characterization of NPs and NP-drug complexes*

The iron-oxide nanoparticles were prepared by alkaline co-precipitation method. The surface of the nanoparticles was modified by coating with polyvinyl pyrrolidone (PVP) and Polyoxyethylene 25-propylene glycol stearate (POES) [Jayakumar et al., 2009; Divakaran et al., 2011]. Magnetic iron oxide nanoparticles were complexed with BBN (0.5%; 1:1) by sonochemical method and characterized by FTIR, XRD and TEM.

### 3.2.4 *Experiment design*

The Dalton's Lymphoma Ascites (DLA) cells were grown on hind limbs of the animal by transplanting  $5 \times 10^6$  cells/animal. Fourteen days after transplantation, the animals were grouped into five with five animals in each group as described below.

- Group 1 : Control- untreated tumor-bearing animals
- Group 2 : NP-Magnet [tumor-bearing animals orally administered with NP (100mg/kg) and treated with external magnetic field]
- Group 3 : BBN (tumor-bearing animals orally administered with BBN; 100mg/kg)
- Group 4 : NP-BBN (tumor-bearing animals orally administered with NP-BBN complexes; 100mg/kg)
- Group 5 : NP-BBN-Magnet [tumor-bearing animals orally administered with NP-BBN complexes (100mg/kg) and treated with external magnetic field]

The animals were administered with NP-BBN complexes for seven consecutive days.

### 3.2.5 *Tumor regression study*

The thickness of hind limb was measured using Vernier calliper (every third day of previous administration) during drug administration. Tumor volume was calculated as follows,

Tumor radius= radius of tumor-bearing hind limb–radius of normal hind limb

Tumor volume =  $\frac{4}{3}\pi r^3$  where 'r' is the radius.

### 3.2.6 *Alkaline single cell gel electrophoresis*

Alkaline single cell gel electrophoresis (Comet assay) was performed to study cellular DNA damages. Here the cells were embedded on slides, pre-coated with 1% normal agarose. The cellular membranes were lysed by incubating cells in lysis solution. Finally electrophoresis was carried out for 30 minutes (20V). The comet parameters such as percentage DNA in tail, tail length, tail moment and olive tail moment were calculated by using the software CASP [Anderson et al., 1998; Klaude et al., 1996].

### 3.2.7 *RNA isolation*

RNA was isolated from tumor tissues of animals by acid guanidium thiocyanate-phenol-chloroform extraction method [Chomczynski and Sacchi, 1987]. The tissues were homogenized in the presence of solution D (4M guanidium thiocyanate, 25mM sodium citrate, 0.5% N-laurosyl sarcosine and 0.1M 2-mercaptoethanol) and treated with sodium acetate, water saturated phenol and chloroform-isoamyl alcohol. RNA was precipitated by isopropanol treatment and washed with 75% ethanol. RNA is solubilised in sterile milli Q water and quantified by taking the absorbance at 260nm.

### 3.2.8 *Polymerase Chain Reaction*

The conventional RT-PCR and qRT-PCR were performed on tumor tissues to identify the changes in the expression of genes such as *bax*, *bcl2* and *caspases 3, 8 and 9* which relate to the apoptotic cell death mechanism. Agarose gel electrophoresis of the RT-PCR product was carried out for 1hr at 10V/cm. The RTq-PCR data was used to calculate relative fold change in the expression of genes in comparison with the untreated control (the expression of  $\beta$ -actin was used as positive control) to indicate the down and up-regulation of the genes- *bax*, *bcl2* and *caspases*. The comparative  $C_T$  method was used to calculate relative fold change in the expression of genes [Thomas and Kenneth, 2008]. The primers used for the study were listed in chapter III.

### 3.2.9 *Morphology analysis*

The tissues such as tumor, liver and kidney were excised and histopathology were performed at Pathology Laboratory, Pushpagiri Institute of Medical Sciences and Research Centre, Tiruvalla, Kerala, India [Culling, 1974].

### 3.2.10 *Hematology studies*

Blood was collected by cardiac puncture and blood count was analyzed by the Mindray auto-hematology analyzer.

### 3.2.11 *Serum biochemical analysis*

Serum levels of urea, creatinine, SGPT, albumin and total protein were analysed in Mispa plus serum biochemical analyzer. The serum urea level was studied by diacetyl monoxime (DAM) reagent method and the serum creatinine level was determined by alkaline picric acid method [Kassirer, 1971; Allen, 1982]. Serum albumin level was determined using bromcresol green [Doumas, 1971], total protein level was found out using a colorimetric method proposed by Hentry (1964) and the SGPT level was determined by the method of Henry et al, 1974 (Agappe Diagnostic Pvt. Ltd.; Ernakulam, Kerala, India).

### 3.2.12 *Statistical analysis*

The results were presented as Mean  $\pm$  SD and were analyzed by GraphPad PRISM software version 5. Statistical analyses of the results were performed using One-way analysis of Variance (ANOVA) with Tukey-Kramer multiple comparisons test.

## 3.3 RESULTS AND DISCUSSION

### 3.3.1 *X-ray diffraction*

Figure 3.1 shows the XRD pattern of the samples, which is quite identical to magnetite ( $\text{Fe}_3\text{O}_4$ ). These peaks obtained were well matched with those of  $\text{Fe}_3\text{O}_4$  (JCP2.2CA:01-089-3854) and the peaks are broadened due to the small size of the particles. The sizes of the particles were calculated by using Scherrer equation and the size varies from  $\sim 7$  to 45 nm (below 50nm) according to the analyses based on the respective (311) peaks.

### 3.3.2 *Infra-Red (IR) spectroscopy*

The various absorption peaks in the IR spectrum have been used for the characterization of  $\text{Fe}_3\text{O}_4$  nanoparticles and NP-drug complexes. The peaks observed at  $3151\text{cm}^{-1}$ ,  $3468\text{cm}^{-1}$  and  $3660\text{cm}^{-1}$  (figure 3.2a, 3.2b and 3.2c) were indicated the presence of -OH group. The peak observed at  $2841.03\text{cm}^{-1}$  in figure 3.2b pointed out the methoxy group in BBN. In figure 3.2b two strong peaks at  $1104$  and  $1029\text{cm}^{-1}$  in the spectrum correspond to the aromatic C-H groups in-plane bend and the peak at  $1508\text{cm}^{-1}$  may correspond to aromatic ring stretch (C=C-C). In the spectrum of NP-BBN complexes (figure 3.2c) it is possible to identify the specific peaks of both NP and BBN.

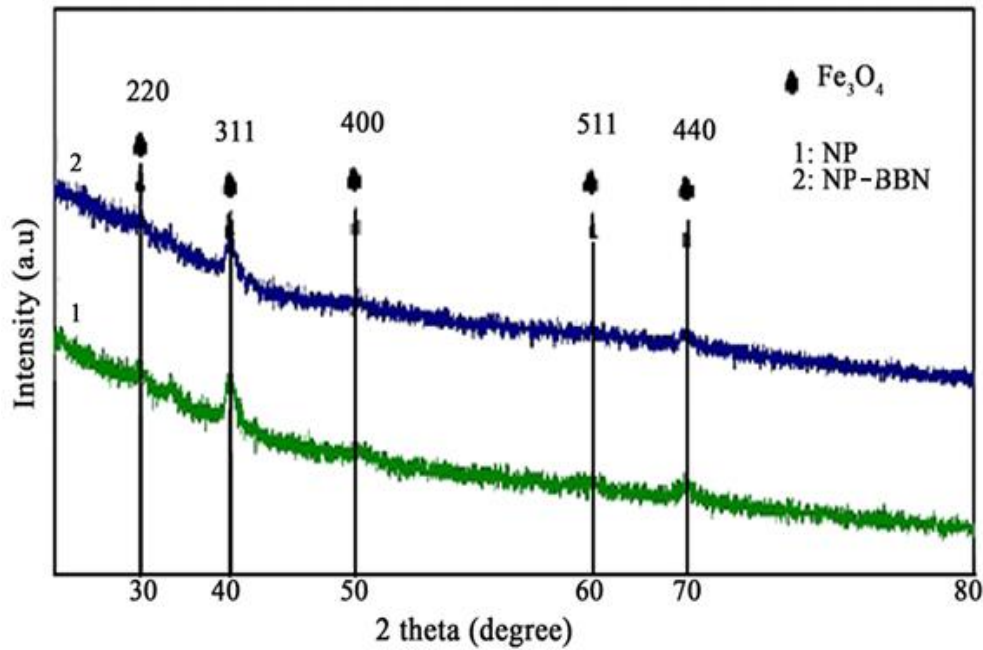


Figure 3.1: XRD pattern of NP (1) and NP-BBN complexes (2).

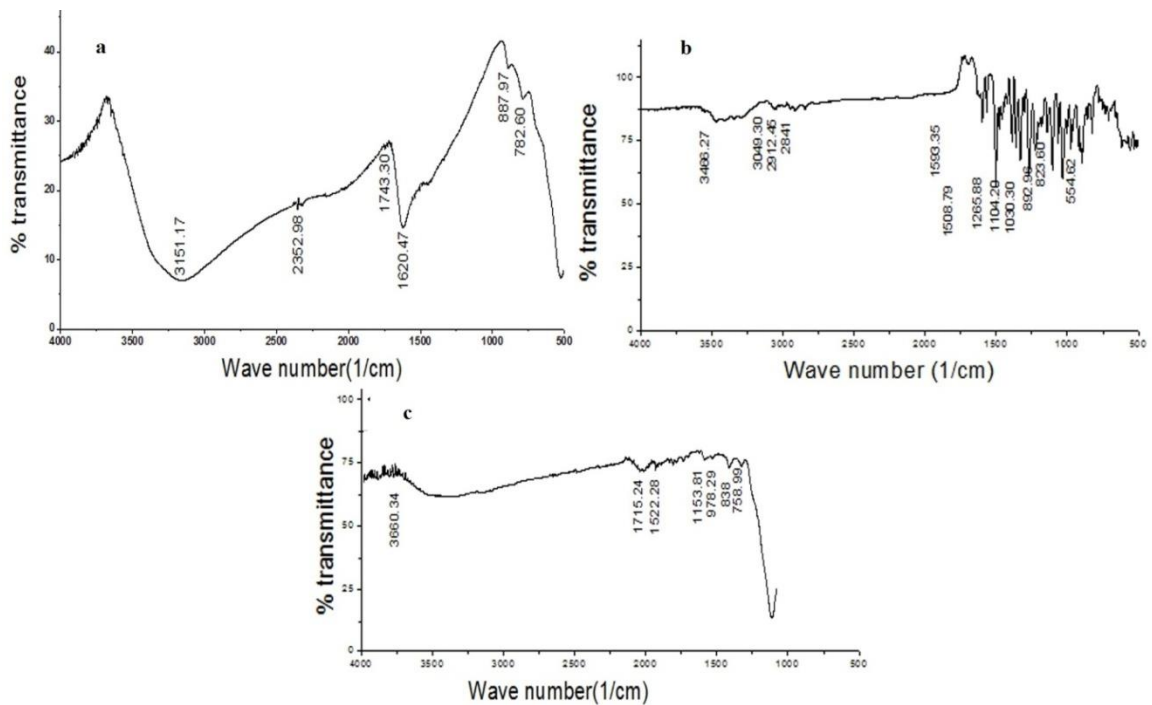


Figure 3.2: FTIR spectra of NPs, drug and NP-drug complexes. a) NPs b) BBN c) NP-BBN complexes.

### 3.3.3 Transmission Electron Microscopy

TEM micrographs were used to learn about the particle size and surface morphology of NPs. The TEM images in figure 3.3c and 3.3d indicated that the size of the particle alone and NP- BBN complexes were less than 50nm.

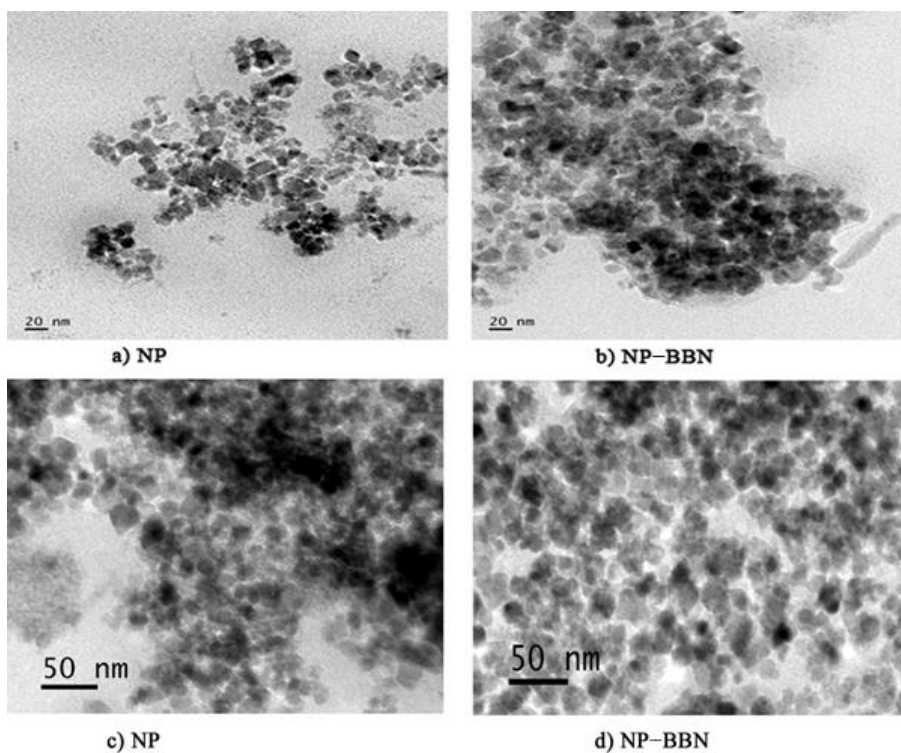


Figure 3.3: TEM images of iron oxide nanoparticles and NP-drug complexes.

### 3.3.4 Analysis of tumor volume following the treatments to understand the anti-neoplastic activity of the treatments

Tumor volume was calculated, as described in the materials and methods, and presented the data in (figure 3.4).

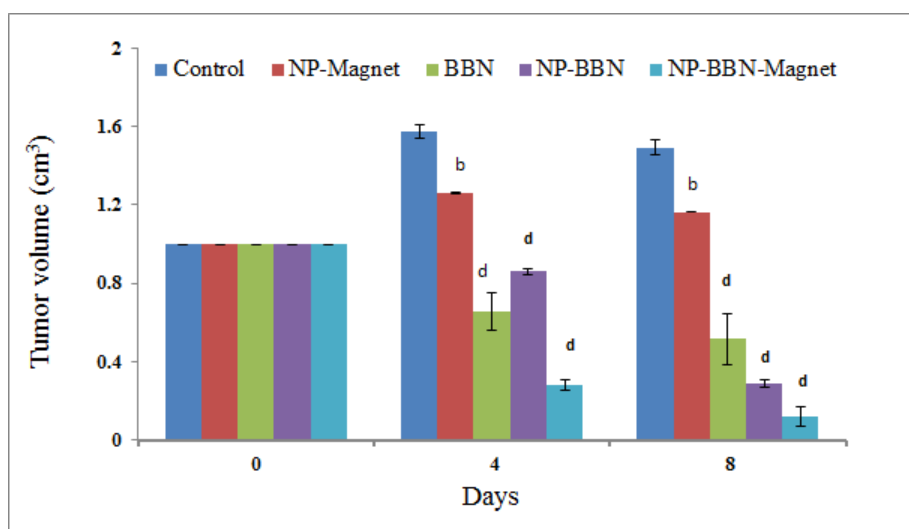


Figure 3.4: Tumor volume following various treatments. Note: ‘b’ indicates  $p < 0.05$  and ‘d’ indicates  $p < 0.001$  when compared with respective control (tumor-bearing, untreated).

It was found that the tumor volume was reduced from  $1\text{cm}^3$  to  $0.121\pm 0.003\text{cm}^3$  in animals administered with NP-BBN complexes and treated with the external magnetic field when compared to control and other treatments, even after seven days of drug administration.

### 3.3.5 Cellular DNA damage analysis on tumor, liver and blood

Alkaline single cell gel electrophoresis (Comet assay) was employed to monitor the extent of cellular DNA damage or DNA degradation by apoptosis in tumor tissues of animals administered with NP-BBN complexes and treated with the external magnetic field. The representative comet pictures of cellular DNA from tumor and normal tissues of the animals following various treatments are presented in figure 3.5. It can be seen that the comet from the tumor tissues of animals treated with either BBN complexed with NP or NP-BBN complexes together with an external magnetic field appeared in fan shape, indicating apoptosis (figure 3.5A).

The comets from the control group did not show comet profile. It is interesting to note that the liver tissue (figure 3.5B) and blood cells (figure 3.5C) of animals did not exhibit any fan shaped comet, indicating no DNA damage or DNA degradation in normal cells following the treatment with NP-BBN complexes and magnetic field.

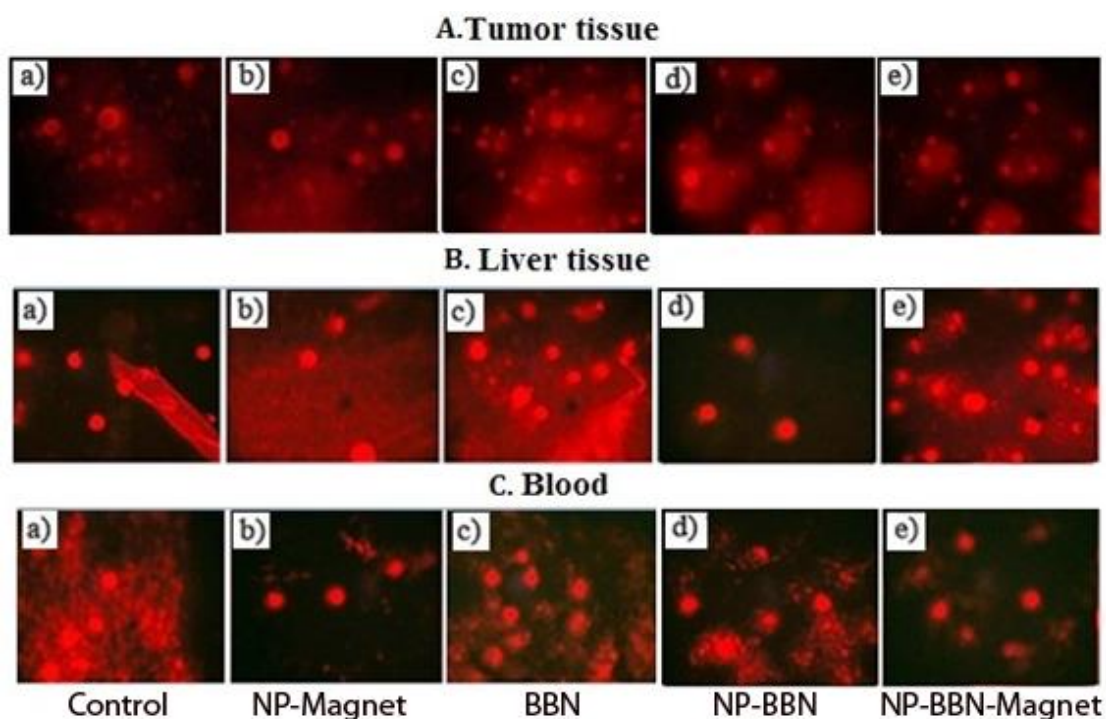


Figure 3.5: Comet images of Tumor (A), Liver (B) and Blood (C).

The comet parameters such as %DNA in tail, Tail length, Tail moment and Olive tail moment were also increased in tumor tissues in NP-BBN-Magnet treatment (figure 3.6).

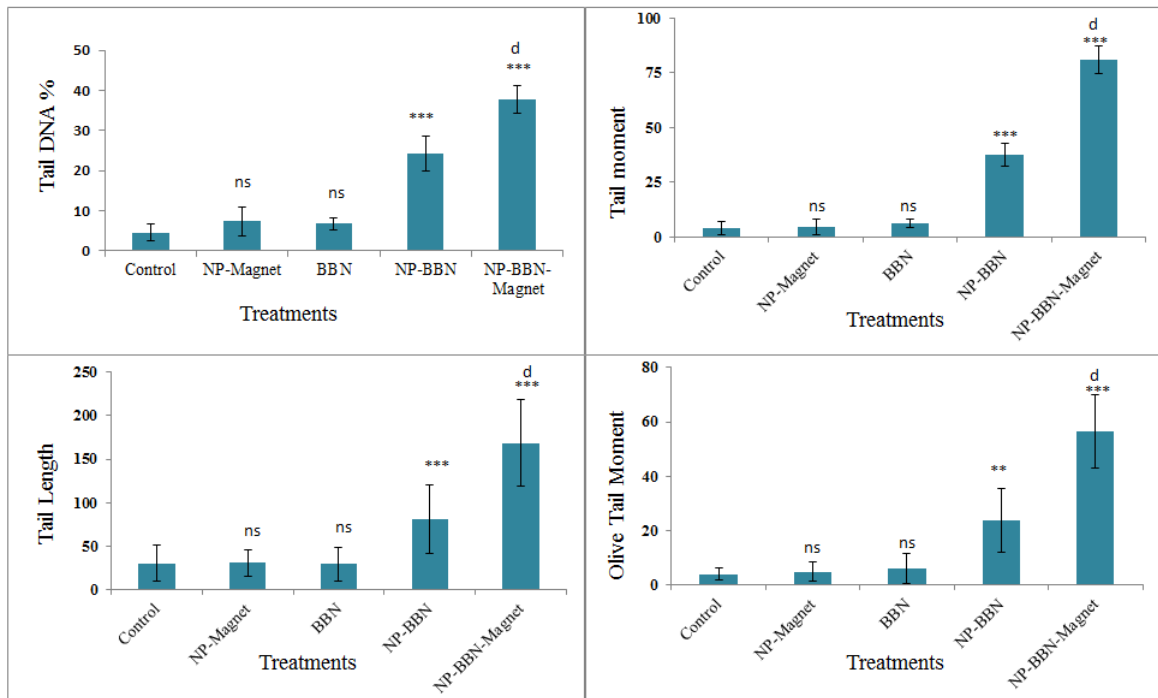


Figure 3.6: Comet parameters of tumor tissues. Note: ‘ns’ indicates non- significance,  $p > 0.05$ ; ‘\*\*\*’ indicates  $p < 0.01$  and ‘\*\*\*’, ‘d’ indicates  $p < 0.001$  when compared with respective controls (control- untreated and NP-BBN complexes).

### 3.3.6 Analysis on the Transcriptional level expression of genes related to apoptosis following the treatments

The expression of genes involved in apoptotic cell death was studied by PCR using specific primers listed in chapter II. Agarose gel electrophoresis was carried out to visualize amplicons and representative images are presented in figure 3.7.

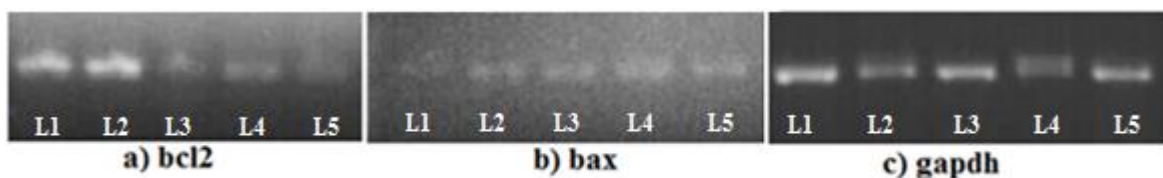


Figure 3.7: Images of agarose gel electrophoresis in tumor tissues. a) anti-apoptotic gene *bcl2*, b) apoptotic gene *bax*, and c) house-keeping gene *gapdh* Note: L1: Control; L2: NP-Magnet; L3: BBN; L4: NP-BBN; L5: NP-BBN-Magnet

From the gel images, it can be seen that there was an up regulation in the expression of gene promoting apoptosis such as *bax* and down regulation of anti-apoptotic gene such as *bcl2* in tumor tissues of animals administered with NP-BBN complexes and treated with external magnetic field. The gene glyceraldehyde-3 phosphate dehydrogenase (*gapdh*) was used as positive control for this study.

The relative expression of genes involved in apoptosis- *bax*, *bcl2*, *caspase 9*, *caspase 8* and *caspase 3* were studied by extracting mRNA from the tumor of the animals following various treatments. From the mRNA, cDNA was synthesized and RTq-PCR was carried out. The data on relative fold change in the expression of these genes with reference to  $\beta$ -*actin* is presented in figure 3.8.

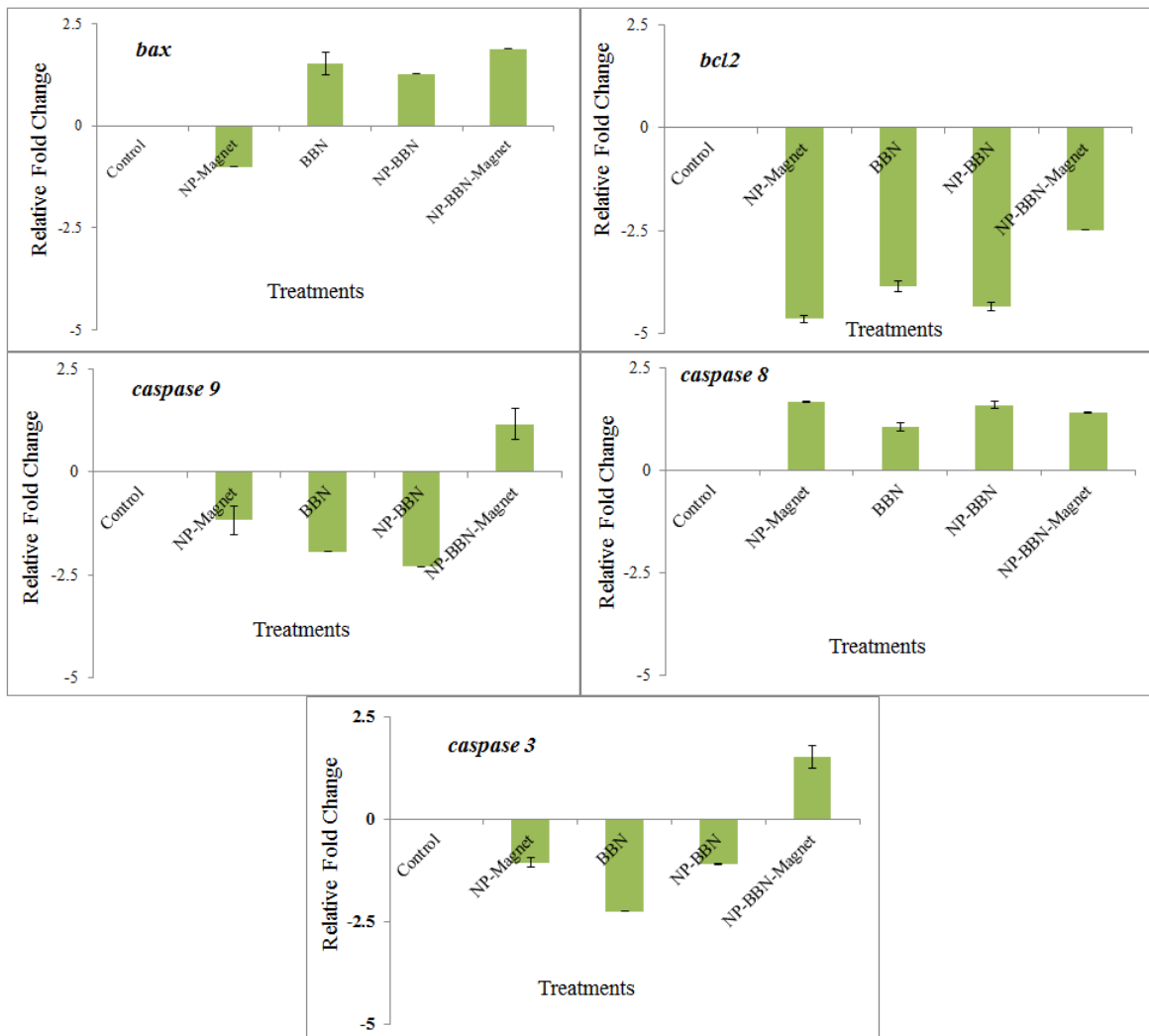


Figure 3.8: Relative fold change in the transcription of various genes related to apoptosis.

Note: The values were expressed as mean $\pm$ SD.

It can be seen in the figure that there was a two-fold increase in the expression of *bax* gene in NP-BBN complexes and magnetic field treated animals compared to the control. Also *bcl2* was decreased in the treated animals compared to the control. These data corroborated the fact that the higher ratio of *bax*-to-*bcl2* is an important marker for apoptosis.

In case of *caspases*, it can be seen that *caspase 8* is expressed in the tumor tissues following all the treatments. This would suggest that the apoptotic pathway in the tumor could be through *caspase 8* to *caspase 7*. However, the animals treated with NP-BBN complexes and external magnetic field, there was up-regulation of *caspase 9* and *caspase 3* while in the other treatment cases these genes were down-regulated, indicating the absence of *caspase 9* to *caspase 3* pathway. This would suggest that the apoptotic pathway of *caspase 9* to *caspase 3* also occurs in animals treated with NP-BBN complexes and external magnetic field in addition to *caspase 8* to *caspase 7* pathway.

### 3.3.7 Analysis on histopathology of tumor and normal tissues

Figure 3.9 gives the histopathological alterations of tumor tissues following the treatment with NP-BBN complexes along with the external magnetic field. Tumor histology of control animals showed large number of pleomorphism as a sign of healthy cancer cells. The cells with condensed nuclei (apoptosis) and anucleated cells (necrosis) can be seen in NP-BBN complexes and magnetic field treated tissues of animals. The normal tissues like kidney and liver did not display any morphological alterations in these treated animals (figure 3.10).

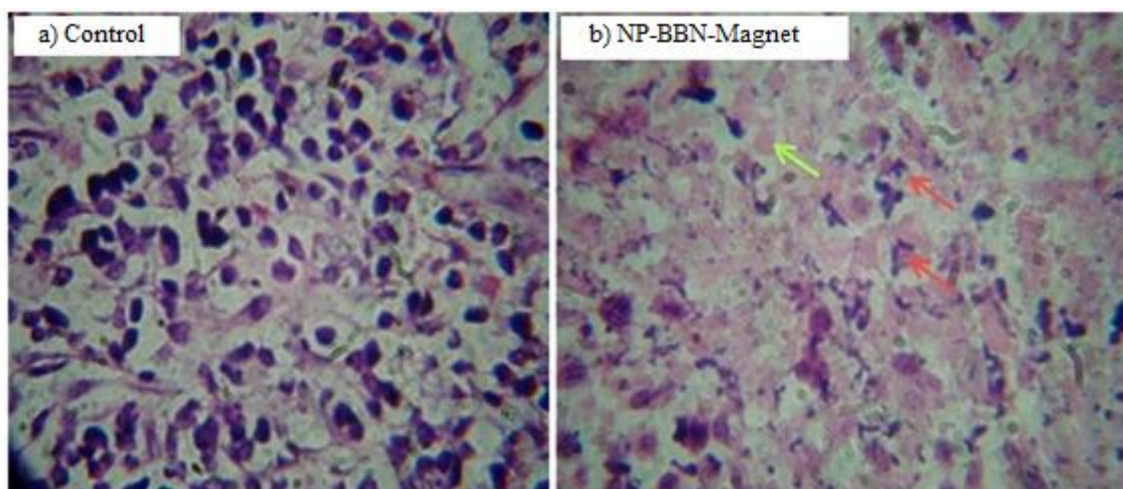


Figure 3.9: Histopathology of tumor tissue. Red coloured arrows indicate apoptosis and green coloured arrow indicates necrosis.

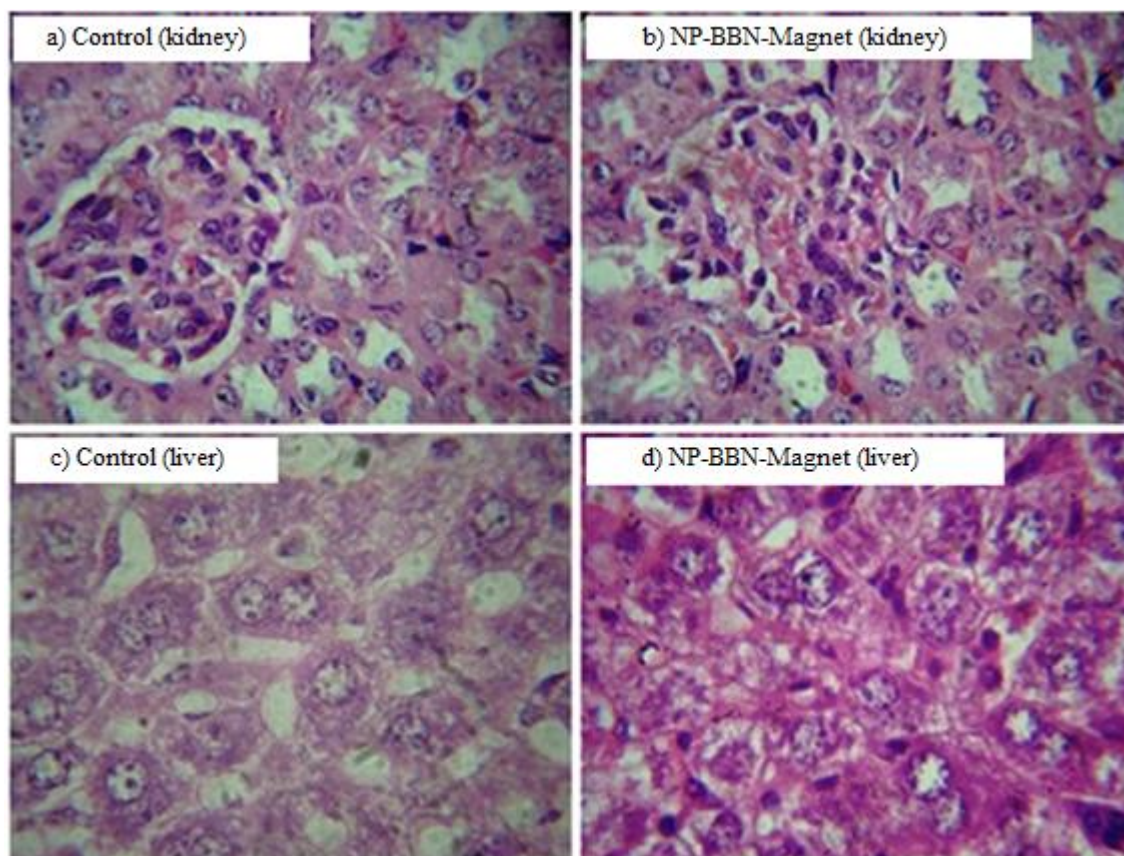


Figure 3.10: Histopathology of kidney and liver (40X magnification).

### 3.3.8 Assessment on blood parameters of animals

The data presented in table 3.1 shows that there was no significant variation after treatment with NP-BBN complexes and external magnetic field in blood cell count compared to the control animals, indicating non-toxicity in these treatments.

Table 3.1: Various hematology parameters following the treatments

Treatments	WBC ( $10^9/L$ )	RBC ( $10^9/L$ )	Platelet ( $10^9/L$ )
Control	$10.35 \pm 0.1$	$8.69 \pm 0.1$	$517 \pm 13.4$
NP-Magnet	$10.0 \pm 0.7$ <sup>ns</sup>	$11.66 \pm 0.9$ <sup>ns</sup>	$636 \pm 4.1$ <sup>**</sup>
BBN	$19.15 \pm 2.2$ <sup>**</sup>	$11.64 \pm 0.5$ <sup>ns</sup>	$727 \pm 4.3$ <sup>***</sup>
NP-BBN	$14.45 \pm 4.5$ <sup>ns</sup>	$10.91 \pm 0.8$ <sup>ns</sup>	$761 \pm 12.3$ <sup>***</sup>
NP-BBN-Magnet	$13.5 \pm 8.4$ <sup>ns</sup>	$10.43 \pm 0.6$ <sup>ns</sup>	$566 \pm 10.5$ <sup>*</sup>

WBC: white blood cells, RBC: red blood cells. Note: ‘ns’ indicates  $P > 0.05$  (non-significant), ‘\*’ indicates  $P < 0.05$ , ‘\*\*’ indicates  $P < 0.01$  and ‘\*\*\*’  $P < 0.001$  when compared with untreated control animals.

### 3.3.9 Serum biomarkers of kidney and liver

As can be evidenced from the data presented in table 3.2, the parameters of serum urea and creatinine levels were in the normal range as compared to the controls, suggesting the absence of renal toxicity. Similarly, serum SGPT and total protein levels were also in the normal range in treated animals compared to control indicating the absence of hepatic toxicity (table 3.3).

Table 3.2: Levels of urea and creatinine in serum

<b>Treatments</b>	<b>Urea (mg/dl)</b>	<b>Creatinine (mg/dl)</b>
Control	44.04 ± 5.9	0.53 ± 0.07
NP-Magnet	50.9 ± 8.3 <sup>ns</sup>	0.42 ± 0.03 <sup>ns</sup>
BBN	54.88 ± 11.9 <sup>ns</sup>	0.28 ± 0.08 <sup>*</sup>
NP-BBN	36.18 ± 2.6 <sup>ns</sup>	0.49 ± 0.01 <sup>ns</sup>
NP-BBN-Magnet	32.72 ± 8.9 <sup>ns</sup>	0.35 ± 0.18 <sup>ns</sup>

Note: ‘ns’ indicate P>0.05 (non-significant) and ‘\*’ indicate P<0.05 when compared with untreated control animals.

Table 3.3: Levels SGPT and Total protein in serum

<b>Treatments</b>	<b>SGPT (U/L)</b>	<b>Total Protein (g/dl)</b>
Control	60.85 ± 1.9	6.38 ± 1.2
NP-Magnet	42.88 ± 20.8 <sup>ns</sup>	6.72 ± 0.7 <sup>ns</sup>
BBN	65.6 ± 3.6 <sup>ns</sup>	5.50 ± 0.8 <sup>ns</sup>
NP-BBN	27.87 ± 4.7 <sup>**</sup>	6.20 ± 0.3 <sup>ns</sup>
NP-BBN-Magnet	53.48 ± 3.8 <sup>ns</sup>	5.40 ± 1.2 <sup>ns</sup>

Note: ‘ns’ indicate P>0.05 (non-significant) and ‘\*\*’ indicate P<0.01 when compared with untreated control animals.

### 3.4 CONCLUSION

The tumor targeted delivery of the drugs can be done by exploiting the magnetic property of iron-oxide nanoparticles [Tietze et al., 2015]. In the present study, we could target the cytotoxic drug BBN, a potent anticancer agent with potent cytotoxic and anti-proliferative activity, to solid tumor in conjugation with magnetic iron-oxide nanoparticles by the help of locally applied external magnetic field. The magnetic field directed accumulation of NP-BBN complexes at the tumor site preferentially, causing cytotoxic effect in tumor cells resulting tumor regression. The administration of BBN alone as well as NP-BBN complexes without magnetic field were not much effective in controlling tumor growth. There was significant up-regulation of the genes involved in apoptosis - *bax*, *caspase 9*, *caspase 8* and *caspase 3* - in tumor of animals treated with magnetic field after administering NP-BBN complexes. The morphological changes in tumor tissues, especially apoptosis, further confirm the observations from the transcriptional expression of the genes. This would suggests the underlying mechanism of toxicity to cancer cells and tumor regression is through caspase-dependent apoptotic pathway. The histopathology of normal tissues and serum biochemical parameters authenticate the specificity of the present treatment approach.